Applied Energy 351 (2023) 121805

Contents lists available at ScienceDirect

Applied Energy

journal homepage: www.elsevier.com/locate/apenergy

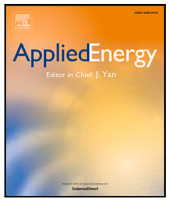

Engine preheating under real-world subfreezing conditions provides less than expected benefits to vehicle fuel economy and emission reduction for light-duty vehicles

Miska Olin [a,b,*], Ville Leinonen [c], Sampsa Martikainen [a], Ukko-Ville Mäkinen [a], Henri Oikarinen [c], Santtu Mikkonen [c,d], Panu Karjalainen [a]

[a] Aerosol Physics Laboratory, Tampere University, Tampere, Finland
[b] Department of Atmospheric Sciences, Texas A&M University, College Station, TX, United States
[c] Department of Technical Physics, University of Eastern Finland, Kuopio, Finland
[d] Department of Environmental and Biological Sciences, University of Eastern Finland, Kuopio, Finland

ARTICLE INFO

Keywords:
Cold start
Vehicle emission
Particle emission
Real-world driving
Subfreezing conditions

ABSTRACT

Six light-duty vehicles, both gasoline- and diesel-fueled, were driven a prescribed 13.8 km route in a real-world low-traffic environment under Finnish subfreezing winter conditions (−28 … −10 °C). Cold starts, hot starts, and starts with different preheating strategies were used. Fuel consumption and emissions of particles and nitrogen oxides (NO_x) were examined by a chasing method with a mobile laboratory. Both electric preheaters (0.3–1.2 kW) and fuel-operated auxiliary heaters (5 kW) were used in the experiments where a cold engine was preheated before starting. While most vehicles showed potential for reducing fuel consumption and emissions of particles (PM), black carbon (BC), and NO_x during hot starts compared to subfreezing-cold starts, the benefits of preheating were relatively small and limited to only a few vehicles. The fuel consumption for the 13.8 km drive decreased less than 4% with one gasoline vehicle and one diesel vehicle by preheating. These two vehicles are both equipped with a fuel-operated auxiliary heater, and taking the fuel consumption of the heater during preheating into account leads to about 30% higher total fuel consumption, canceling the preheating benefit out. These two vehicles also showed the largest reductions in PM, BC, and NO_x emissions achieved with preheating, e.g., the PM emission reductions being 72% (the gasoline vehicle) and 24% (the diesel vehicle). Whereas the NO_x emission reduction for this gasoline vehicle was 41% when considering only the drive, it decreases to 15% when the NO_x emissions from the auxiliary heater during preheating are also taken into account. High particle number (PN) emissions from all vehicles and NO_x emissions from the diesel vehicles were detected. The PN emissions of particles larger than 23 nm were up to 2 orders of magnitude higher and the NO_x emissions up to a factor of 21 higher than the corresponding limits in the European regulations for type-approval of new vehicles. The PN emissions did not depend on the start types; thus, no benefits to reduce them with preheating were detected. The limit-exceeding PN emissions are partially explained with the used measurement method for PN taking both nonvolatile and semivolatile particles into account, whereas the regulations take only the nonvolatile particles into account. The PM emissions were also observed to consist mostly of semivolatile material in most of the cases, organics being the main component of the semivolatile material.

1. Introduction

Road traffic is one of the main sources of emissions worsening air quality and being detrimental to human health. The highest ambient particle concentrations have been observed at locations with dense traffic, such as on highways, on streets (e.g., Kittelson et al. [1]), and in street canyons (e.g., Wehner et al. [2], Hietikko et al. [3], Olin et al. [4], Olin et al. [5], Lintusaari et al. [6]).

Many particle and gas phase emissions, such as particle mass (PM), total hydrocarbons, nitrogen oxides (NO_x), and carbon monoxide, have been regulated in many countries for newly sold vehicles [7]. PM emission limits were introduced in the Euro 5 level for both diesel and gasoline vehicles with the limit of 5 mg/km in type-approval tests. As for particle emissions, in addition to PM, also particle number (PN) emissions have been regulated since the Euro 5b emission level for

* Corresponding author at: Department of Atmospheric Sciences, Texas A&M University, College Station, TX, United States.
E-mail address: miska.olin@tamu.edu (M. Olin).

https://doi.org/10.1016/j.apenergy.2023.121805
Received 11 May 2023; Received in revised form 13 August 2023; Accepted 17 August 2023
Available online 30 August 2023

light-duty vehicles but considering only nonvolatile particles. This PN emission limit (6×10^{11} #/km in chassis dynamometer tests) applies also to gasoline vehicles which are equipped with gasoline direct injection (GDI) since the Euro 6c emission level, but a higher limit (6×10^{12} #/km) is allowed for Euro 6b gasoline vehicles.

In addition to the current PN emission regulations focusing only on nonvolatile particles, they also consider only particles larger than 23 nm. However, the existence of the both particle volatility types (nonvolatile and semivolatile) and sub−23 nm particles in vehicle exhaust is expected, and the real-world particle emissions can hence differ greatly from the regulated ones [8]. The regulated particle emissions include basically only primary particle emissions, which are particles formed during the combustion process and are mostly nonvolatile. Those are chosen for the regulations due to better repeatability of determining emissions of >23 nm nonvolatile particles in laboratory settings. After the exhaust has been released from the tailpipe, rapid cooling of the exhaust plume tends to both form new particles via nucleation and to grow the existing and the newly formed ones via condensation with low-volatility vapors [9]. This add-on to the primary particle emissions, called delayed primary emissions [10], typically consists mainly of semivolatile particle material.

Particle emission control of diesel vehicles has, already for several years, been achieved with de facto enforcing diesel particle filters (DPFs) in the majority of diesel applications. DPFs effectively filter the exhaust from particles before it is emitted to the atmosphere and have been shown to reduce real-world PM emissions by at least 90% and PN emissions even more [11–13], even down to the detection limits of particle counters. Due to the general need to enhance the fuel economy, use of GDI in gasoline vehicles has been increased [14], which has, in turn, increased particle emissions of the gasoline vehicle fleet [15–17]. Hence, gasoline particle filters (GPFs) have also become applied in modern gasoline vehicles.

NO_x emissions have mainly been a problem with diesel vehicles due to their higher combustion temperature. These emissions have, nevertheless, been reduced in practice with exhaust gas recirculation (EGR) systems and nowadays also with selective catalytic reduction (SCR) systems. These systems are, however, prone to end user manipulation but also to manipulation performed already by the manufacturers, such as in the Dieselgate scandal. The most recent emission regulation levels (Euro 5 and 6) limit the NO_x emissions to 60 mg/km for gasoline vehicles, to 180 mg/km for Euro 5 diesel vehicles, and to 80 mg/km for Euro 6 diesel vehicles.

Cold-starting a vehicle is known to emit more pollutants during the first minutes of operation [18], mainly due to time required for the catalytic converter to be warmed up to its operation temperature. Especially concentrations of organic compounds can be orders of magnitude higher in the exhaust during a cold start compared to the warm operation of the same vehicle [19,20] but also NO_x, PM, and carbon monoxide emissions are higher during cold starts [18]. For these reasons, the vehicle emission regulations try to include the cold start emissions in their type-approval tests. The definition of a cold start varies between the governing regulations worldwide, but it is typically related to the soak time (e.g., at least 1 h) or to the coolant temperature (e.g., below 35 °C or below T+10 °F), where T denotes the ambient temperature.

In addition to increased emissions during a cold start, the fuel consumption is also increased and is dependent on T [21–23]. One reason is that colder lubricant having a higher viscosity leads to increased friction in the engine and thus to increased fuel consumption [24]. Moreover, a significant fraction of energy from combustion is lost due to heat conduction into the cold metallic parts of the engine, further increasing fuel consumption.

Most of the previous research on cold start emissions and fuel consumption, however, focus on ambient temperatures higher than 0 °C; even 20 °C is considered a cold start in many contexts. However, in high altitude or mountain regions, such as in Scandinavia or in northern parts of North America, temperatures frequently fall below 0 °C (denoted here as subfreezing conditions) during wintertime. Since the daily minimum temperatures are below 0 °C roughly for the half of the year in Scandinavia, operating vehicles under subfreezing conditions is noteworthy because the first ignition of a vehicle usually occurs in the mornings, where the ambient temperature is typically at its lowest. Additionally, previous studies are mainly performed as laboratory tests where the studied vehicle is on a dynamometer and a prescribed driving cycle is driven rather than driving the vehicle in a real-world environment.

Common solutions to prevent excessive wear on the engine during a cold start and to lengthen the life time of the lubricant under subfreezing conditions in Scandinavia are preheaters or auxiliary heaters (AHs). They also ensure that the engine starts better at very low temperatures and help with heating up the cabin air—and therefore with melting ice from the windows—but are also traditionally justified in providing benefits to fuel economy and emission reduction. These heaters use either fuel or electricity to generate the needed heat. Electric heaters can only be used as preheaters since they require a connection to the power grid but the fuel-operated heaters can act both as preheaters and AHs. This means that an AH can, firstly, heat the engine and the cabin air before starting the engine and, secondly, output some additional heat needed for reaching faster and maintaining the operation temperature of the engine during driving in a very cold environment. The heat produced by an AH in light-duty vehicles is always transferred to the engine and to the cabin via circulated coolant, but the electric preheaters heat directly the engine block, coolant (either with circulation or without), or lubricant. Additionally, separate electric cabin preheaters exist which, if equipped, are commonly used together with the electric engine preheaters. Nowadays also electric heat pump systems have become more common with the electrification of the vehicle fleets, which are typical for fully electric vehicles. However, plug-in hybrid electric vehicles (PHEVs) can still be equipped only with fuel-operated heaters although they can be driven with only using electricity.

Whereas the heating power of electric preheaters are typically below 0.5 kW, fuel-operated AHs heat typically with the power of 5 kW. Traditionally the share of electric preheaters in light-duty vehicles in Scandinavia has been higher than of fuel-operated AHs. However, the share of AHs has been increased during the last decade—also, e.g., in Central Europe—due to the general need to enhance the fuel efficiency, which has led to fewer amounts of excess heat generated by the engines. Since AHs are always operated with fuel and they have a separate exhaust pipe (not including any exhaust after-treatment systems) from the tailpipe, also their fuel consumption and emissions need to be considered in full perspective. Research on AH emissions has been very scarce in the past. Only very recently [25,26], their emissions have been found to be substantial and higher than the emissions from the engines. Due to the constantly increasing share of fuel-operated AHs and their observed emission concerns, their usage needs to be re-assessed. This also applies to electric preheaters due to the recent steeply risen electricity prices in Europe.

Rautalin [27] and Rautalin and Nuottimäki [28] studied the effect of preheaters (both electric and fuel-operated) on gasoline and diesel passenger car fuel consumption and PM, NO_x, carbon monoxide, and hydrocarbon emissions in an engine dynamometer laboratory (NEDC cycle) in temperatures of −20, −7, and 0 °C. They concluded that whereas the potential for decreased fuel consumption (the decreased fuel consumption when comparing cold and hot starts) is on the order of 30% for the first 4 km driven, the fuel consumption decreased 2.7%–16% with using a preheater, for the first 4 km driven, in temperatures of −20 and −7 °C, the largest decreases being for a vehicle having a fuel-operated preheater. The decrease of PM emissions due to a preheater (in temperatures of −20 and −7 °C) for the first 4 km driven was 42%–78% for gasoline vehicles. For diesel vehicles, the PM emissions were close to the detection limit due to their equipped DPFs. No clear effect on the NO_x emissions because of preheaters were observed. The effect

Table 1
Details of the studied vehicles. * denotes a particle filter (DPF/GPF) and † denotes a SCR system.

Make and model	Fuel	First registration year	Emission level	Engine model	Engine power (kW)	Odometer reading (km)	Preheater power (kW) and type
Ford Focus	Gasoline	2018	Euro 6	1.0 EcoBoost	74	78,000	0.3, Electric
Skoda Octavia 1	Gasoline	2020	Euro 6*	1.0 TSI MHEV	81	1,000	5.0, Fuel
Skoda Octavia 2	Gasoline	2019	Euro 6*	2.0 TSI	140	21,000	5.0, Fuel
Audi A6	Diesel	2008	Euro 5*	3.0 TDI	176	236,000	1.2, Electric
SEAT Alhambra	Diesel	2012	Euro 5*†	2.0 TDI	103	169,000	5.0, Fuel
VW Transporter	Diesel	2019	Euro 6*†	2.0 TDI	75	36,000	0.3, Electric

of temperature on fuel consumption for the whole 11 km driving of the NEDC cycle was about −0.8%/°C, denoting that the fuel consumption was 0.8% lower for every additional °C. This applies to both diesel and gasoline vehicles and to both cold starts and preheated starts. This value for the PM emissions from gasoline vehicles was from −0 to −3%/°C. Corresponding values for the NO_x emissions were about −2%/°C for the gasoline vehicles and from −0 to −3% for the diesel vehicles.

Similarly, Rautalin [29] studied the effect of 0.6 kW electric preheaters (together with separate 1.9 kW cabin heaters) in gasoline and diesel passenger cars and concluded that the fuel consumption for the whole NEDC cycle (T = −20 °C) decreased about 20%–30% because of preheating. The NO_x emissions decreased about 40%–50% and the decreases of PM, carbon monoxide, and hydrocarbons were, within the accuracy of the measurement, close to 100%.

The previously mentioned studies [27–29] reach temperatures down to −20 °C, but are, however, all conducted in a laboratory rather than in real-world settings. The effects of preheaters and T especially on emissions may differ substantially between laboratory and real-world settings. This is because, e.g., the delayed primary emissions formed upon the exhaust cooling when released from the tailpipe is not easily mimicked with any laboratory system. A common problem with laboratory systems trying to mimic this exhaust cooling is that they do not usually apply dilution air cold enough, because a high flow of very cold (e.g., −20 °C) dilution air is typically difficult to arrange. However, the effect of T can be substantial in the formation of delayed primary emission because gas-to-particle conversion is generally very strongly dependent on temperature. The previous studies also did not include measurements of delayed primary emissions and the temperature of the dilution air was not reported.

In this study, we examine the role of cold starts and vehicle preheating strategies in the formation of primary and delayed primary emission and fuel consumption under subfreezing conditions in a real-world environment. Altogether six light-duty vehicles (three gasoline and three diesel vehicles) were selected for on-road tests with real-time sampling and instrumentation under Finnish winter conditions (−28 … −10 °C). Different preheaters were included in studies (fuel-operated AHs and electric preheaters). We report the fuel consumption and the emission factors of PN, PM, BC, particle size distributions, particle chemical composition, and NO_x, and discuss different advantages and disadvantages in engine preheating.

2. Methods

2.1. Studied vehicles

Table 1 lists the vehicles used in this study. The details on their fuels, ages, engines, emission controlling, and preheaters are also listed. All the studied vehicles have direct injection techniques. Skoda Octavia 1 is a mild hybrid electric vehicle (MHEV), which denotes a vehicle having only a very small battery for electric operation, and the electric motor is normally used only for giving additional power operated in parallel to the internal combustion engine but also for storing energy from braking. It also cannot be charged with external electricity.

Specific details on the used fuels are not available, since there were vehicles which were rented from car rental suppliers; thus, the history of their refueling was not available. Nevertheless, the fuel grades can be assumed to be typical fuels commercially available in Finland, such as 95E10 for gasoline (max. ethanol content of 10%) and EN590 for diesel.

Three fuel-operated (AHs) and three electric preheaters were used. All the fuel-operated heaters were typical AHs of the same model with the nominal power of 5 kW. Whereas the fuel-operated AHs heat both the engine and the cabin air through the coolant circulated with an external circulation pump, the electric preheaters heat only the engine (no separate electric cabin heaters were used in this study). The electric preheaters of Ford Focus and VW Transporter heat the engine by heating the engine oil externally (without any forced circulation) with the average power of about 0.3 kW, measured with an energy meter installed in the power grid plug. The electric preheater of Audi A6 heats the engine through the coolant that is also circulated with an external circulation pump, and the average power of the heater was about 1.2 kW. Audi A6 was also equipped with a front grille cover, used to prevent undesired cooling of the coolant by the road draft under low ambient temperatures and to make the engine and the cabin to heat up faster during driving.

2.2. Measurement location and protocol

The measurement location was a rural area in Eastern Finland with relatively low population and traffic density. The measurement route is presented in Fig. 1 showing an example of vehicle speeds during the drives. It also shows the location where the drives began and ended and the locations of four artificial stops made to simulate stops possibly occurring in more urban locations caused by, e.g., traffic lights. The route is divided into four parts with slightly different surrounding and road properties (see Table S1 of the supplementary material) for result interpretation purposes.

The experiments were conducted on four consecutive days in February 2021, representing the coldest time of the year. The ambient temperatures during the drives were between −28 and −10 °C. The relative humidity was mainly within 70%–90% and the wind speeds were mostly below 4 m/s. The weather was mostly clear but there was light snowing on the last measurement day.

All the drives for all six vehicles measured were driven similarly with as equal driving speeds, accelerations, and timings as possible in a real-world environment. However, the drives differ from each other in terms of preheating and engine starting. Three different types of engine starts were made:

Subfreezing–cold start (SFCS) without any preheating and starting the engine as cold (after a long soak time)

Preheated–cold start (PHCS) with preheating and starting the engine right after a prescribed heating time

Hot start (HS) after driving one drive and ensuring the engine has reached its operation temperature, and starting the engine again right after that

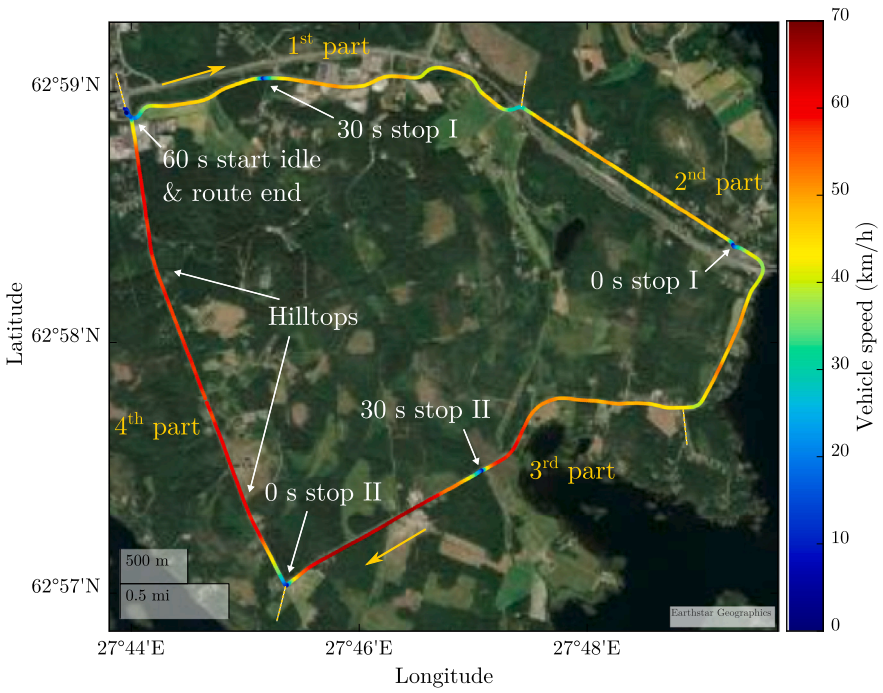

Fig. 1. Summer-time satellite image showing the 13.8 km measurement route colored with an example of vehicle speeds during the drives. The yellow dashed lines denote the boundaries of the four parts of the route, used in result interpretation.

SFCSs and PHCSs are both considered cold starts here because even the coolant temperatures while starting the engines after the preheating periods were relatively low (see Fig. S5 of the supplementary material), mostly below 35 °C, which is one definition for a cold start in the European emission regulations for vehicles. Ford Focus and VW Transporter having electric preheaters with only the power of 0.3 kW had the starting coolant temperatures close to the ambient temperature (see also Fig. S6 of the supplementary material for the effect in comparison to the ambient temperature). The "subfreezing" term is used in SFCS to highlight that T was below typical cold start temperatures in previous literature.

Before the SFCS and PHCS drives, the vehicles were soaking the previous night, which was at least 17 h from the previous driving, except two SFCS drives: one for Skoda Octavia 2 and one for VW Transporter, those having soak times of about 5 h (see Table S2 of the supplementary material). In these exceptional cases, 5 h soak time was assumed enough to cool down the vehicle because of very low T and because the engine hoods were left open to speed up the cooling. This is also verified with the starting coolant temperatures (Figs. S5 and S6 of the supplementary material).

In the experiments where preheating was used (PHCSs), the AHs, if equipped, were run for 30 min (usually a default setting causing an automatic shutdown of the AH after fulfilling the prescribed time period) before starting the vehicle. One exception to this rule was one drive with Skoda Octavia 2, in which the AH was run for 43 min due to the functionality of that vehicle having no automatic AH shutdown and because the previous experiment with another vehicle was still being conducted at the 30 min time moment. A typical heating time of an AH is about 30 min which is usually enough for heating the engine, warming the cabin, and melting the ice from the windows. Additional 13 min of heating is assumed to not make any significant changes in the emissions and fuel consumption during driving. The preheating times with the electric heaters were 67–176 min (see Table S2 of the supplementary material), the longest ones for the 0.3 kW heaters (Ford Focus and VW Transporter). Typical heating times with electric heaters are around 2 h, and longer times are assumed to give no additional benefits with low-power heaters since the thermal loss under subfreezing conditions can be on a similar level to the power of a heater. These preheating times also varied between the drives due to timing of the experiments with other vehicles and because electric preheaters did not have any automatized operation methods. The shortest preheating times (65–106 min) with electric preheaters were used with Audi A6 since it was equipped with the preheater with the highest power (1.2 kW). The other two vehicles having 0.3 kW preheaters (Ford Focus and VW Transporter) were measured with the preheating times of 110–176 min.

All the drives were performed two times, on separate days, to provide some repetitions. However, the usage of Soot Particle Aerosol Mass Spectrometer (SP-AMS) differed slightly between these days (see Section 2.3 for the details). Also, there were problems with some measurement instruments with the HS drive for Ford Focus and the SFCS drive for VW Transporter; thus, these drives are disregarded from the data analysis. The outdoor conditions, however, were slightly different on those days, but that provides also some information on the effect of T on the results. The drives included possible preheating, 1 min idle period after the engine start, approximately 19 min of driving (13.8 km), and 1 min idle period after the drive. The last idle period was not included in the data analysis, however. The first idle period was used to simulate a typical idling time that frequently occurs due to the need to clear the ice and snow from top of the vehicle. For the results interpretation, the experiments are divided into six segments (see Table S1 of the supplementary material): the preheating, the idling, and the four different parts of the route (Fig. 1). The driving speed varied slightly (around 50 km/h) between the parts of the route. The route has some uphill and downhill driving, the tallest two hills being in the 4th part of the route, with about 50 m changes in the elevation to both directions. See Table S1 and Fig. S1 of the supplementary material for more detailed information on the route. In addition to these drives with the studied vehicles, totaling 34 drives, background experiments were also performed once a day, i.e., totaling four times. The background experiments were conducted with measuring the ambient air (see Section 2.3 for the details on how the measurements were performed) without any studied vehicle to enable the detection of the emissions from a specific vehicle (background concentrations subtracted from the measured ones).

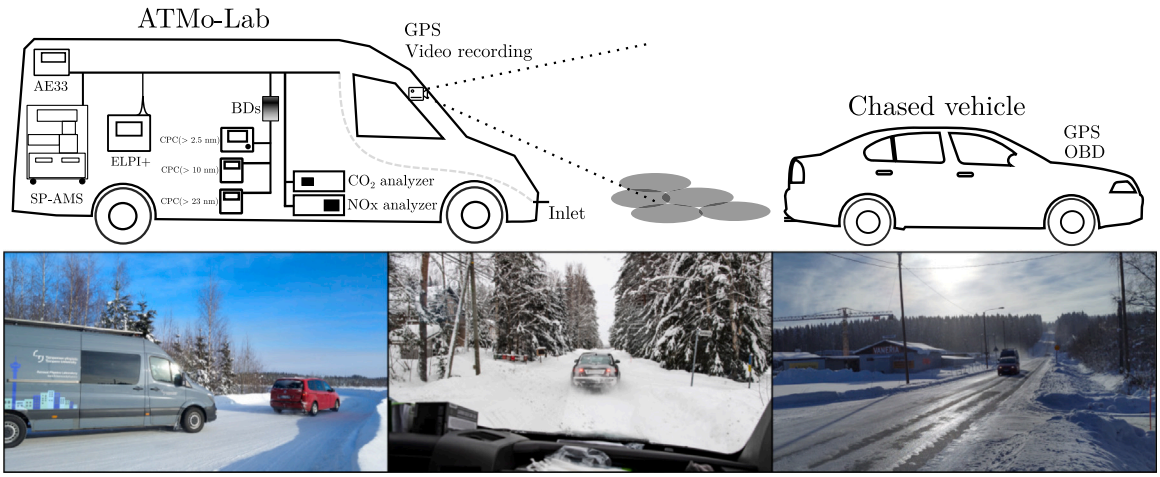

Fig. 2. Measurement setup and sample pictures during the chase measurements. Also other devices were installed but their data are not used in this study.

Whereas the electric preheaters can only be used with a standstill vehicle, the AHs can also heat during driving. Because the automatic operation of the AHs during driving was not possible to alter, they have been running automatically for at least some parts of the drives. Information on their running states during driving were not available for logging. Thus, their operational times during driving are unknown, but it is expected that their running times are the longest for the drives in which preheating was not used, but it is likely that they have been running also during the drives with hot engines as well, due to the very cold conditions in some experiments.

2.3. Measurement setup and data analysis

Fig. 2 presents the measurement setup inside Tampere University's mobile laboratory (Aerosol and Trace gas Mobile Laboratory, ATMo-Lab). ATMo-Lab was used to measure the emissions of the studied vehicles by a chasing method (and also to measure the ambient air in the background experiments). The chasing distance was kept as short as possible but with maintaining necessary driving safety; the distance was approximately 5–10 m when driving, as can be seen from the sample pictures in Fig. 2, but was only about 1 m when stationary.

The measurement devices inside ATMo-Lab included Condensation Particles Counters (CPCs) for the particle number concentrations, an Aethalometer (AE33, Aerosol Co.) for the black carbon mass concentration, an Electrical Low Pressure Impactor (ELPI+, Dekati Ltd) for the particle size distribution and mass concentration, a SP-AMS (Aerodyne Research Inc.) for particle chemical composition, and an infrared gas analyzer for CO_2 (LI-840 A, LI-COR Inc.) concentrations and a chemiluminescence analyzer for NO_x (Model T201, Teledyne Technologies Inc.) concentrations. ATMo-Lab also includes a weather station (Airmar Technology Corp.), which was used to obtain the GPS data, such as speed and location. It also includes a dash camera for video recording during the drives. The chased vehicles also included GPS loggers, and parameters, e.g., from the engine operation and fuel consumption, were logged through their OBD ports. The ambient temperature (T) was obtained from a national weather network station located a few kilometers away from the measurement location.

The different CPCs with different cut-off particle diameters (D_p) were used to obtain also information on the particle size distributions with them, in addition to particle number concentrations (N). The used CPCs were CPC 3756 (TSI Inc.) with the nominal cut-off size of 2.5 nm, CPC A20 (Airmodus Ltd) with the nominal cut-off size of 10 nm, and CPC A23 (Airmodus Ltd) with the nominal cut-off size of 23 nm. Because particle number concentrations in exhaust plumes frequently exceed the upper limits of the CPCs, two bifurcated-flow diluters (BDs) in the front of the CPCs were used to passively decrease the concentrations. These BDs decreased the number concentrations for the CPC with the dilution ratio (DR) of 158 ± 14, determined in a separate experiment with combustion-generated particles.

The exhaust or ambient sample was drawn in ATMo-Lab through the inlet on the front bumper using the suction of the measurement devices. Because the sampling lines and the BDs cause excessive diffusional losses for very small particles (say <10 nm) also with high uncertainties when the losses are corrected using theoretical diffusional correction functions, as is described in Olin et al. [30], the diffusional losses were not corrected in this study. Instead, the cut-off sizes of the used CPCs are here converted to effective cut-off sizes. Whereas the cut-off size of a CPC generally represents D_p where the detection efficiency of the CPC is 50% of the maximum detection efficiency, the effective cut-off size is here defined so that this 50% level is interpreted from the detection efficiency curve of a CPC which is multiplied with the penetration efficiency of the sampling system. In other words, this denotes a cut-off size that would be for a CPC if the sampling lines inside ATMo-Lab were thought to be a part of the CPC. The original and the modified detection efficiency curves for the CPC are presented in Fig. S2 of the supplementary material. In conclusion, the particle number concentrations measured with the CPCs with the nominal cut-off sizes of 2.5, 10, and 23 nm are here considered the number concentrations of particles larger than 6.7, 11.5, and 22.8 nm, respectively.

All the instruments except the SP-AMS logged data on 1 s time resolution. The resolution of the SP-AMS was 23 s. It is based on the high resolution–time-of-flight–aerosol mass spectrometer (HR-ToF-AMS) described by DeCarlo et al. [31] with an additional soot particle (SP) module for detecting black carbon and other refractory species [32]. The data have been analyzed in Wavemetrics Igor Pro 9 using the extensions SQUIRREL (v. 1.65) and PIKA (v. 1.25). The calibrations based on the description by Onasch et al. [32] were used to determine the ionization efficiencies which are applied in the data analysis. The collection efficiencies described by Middlebrook et al. [33] are also calculated and applied. After the data analysis procedures described by DeCarlo et al. [31], the results are divided into groups (particle organics, sulfate, nitrate, ammonium, and chloride compounds) to help to analyze the results.

In this study, the data measured with the AE33 (with the wavelength of 880 nm) are used as the mass concentration of black carbon (BC), instead of the refractory black carbon measured with the SP-AMS. Therefore, the BC data from the AE33 are averaged to the 23 s time bins equal to the time bins of the SP-AMS. This also prevents negative signals from the AE33, which are typically encountered when using the time resolution of only 1 s. Whereas all the other measurement devices except the SP-AMS used in this study involve a repetition experiment performed on another day (see Section 2.2), the SP-AMS data shown

here are only from one experiment (per vehicle per drive type) because the SP-AMS was used for secondary aerosol measurements on those another days, but the secondary aerosol data are out of the scope of this study. This also results in missing SP-AMS-related results for the HS of Ford Focus and the SFCS of VW Transporter, because those were the experiments without any successful repetitions.

The ELPI+ measures the particle size distribution in 14 particle size bins (from 6 nm to 10 μm). This size distribution is denoted here as $\mathrm{d}N(\mathrm{ELPI+})/\mathrm{d}\log D_\mathrm{p}$. For the particle mass concentration (PM), only the first eight bins (from 6 to 600 nm) are used here due to unknown particle density (a unit density is assumed here) causing uncertainties in the data inversion especially in the size bins with the highest particle diameters, and particle emissions of vehicles are typically below 600 nm in D_p anyway. This PM calculated from the data from the first eight bins of the ELPI+ is denoted here as $M(\mathrm{ELPI+})$.

Because the time response of the NO_x analyzer is on the order of 30 s, the recorded data were deconvolved using the Richardson–Lucy deconvolution method with 100 iterations using a previously determined response function as the initial guess for the convolution vector. Because deconvolution generally is not perfect and not outputting a unique result, the data after the deconvolution were averaged to 10 s time resolution to smooth the deconvolved data a bit. The NO_x analyzer (with the used measurement mode) reports the NO_x concentration as the sum of the volumetric concentrations of nitric oxide (NO) and nitrogen dioxide (NO_2) but the vehicle emission regulations are based on the mass concentration of NO_x. Therefore, the recorded data were converted to the mass concentrations by assuming a constant NO_2/NO_x ratio of the emissions. The NO_2/NO_x ratio varies between 10 and 30%, depending on the fuel and model year [34]; a constant value of 25% is used in this study. Although some uncertainty is involved in this value, the contribution of this uncertainty to the reported masses is not major since the molar masses of NO and NO_2 (30 and 46 g/mol, respectively) are not very different.

Emission factors (EFs) are here expressed as cumulative amounts of pollutants emitted until a given driving distance (in km) or as amounts of pollutants emitted per 1 km (calculated as the cumulative EF from the full drive divided by the length of the full drive). A cumulative EFs for a pollutant x for a given driving time $\mathcal{T}$ is calculated using the equation, based on Wihersaari et al. [13],

$$\mathrm{EF}_{x,\mathcal{T}} = \sum_{t=0}^{\mathcal{T}} \underbrace{(x_t - x_\mathrm{bg})}_{\geq 0} \mathrm{DR}_t\, Q_t \tag{1}$$

where x_t and DR_t are the concentration of the pollutant and the dilution ratio, respectively, of the raw exhaust at the distance of the sampling inlet of ATMo-Lab (i.e., of the diluted exhaust) at a given time t; and x_bg and Q_t are the background concentration of the pollutant and the exhaust volumetric flow rate (assuming air density in −10 °C) at a given time t, respectively. The background concentrations, x_bg, are constants within a drive and their values are determined from their median concentrations during the background drives. Because there are some situations where x_bg is higher than x_t, due to the fact that x_bg is not possible to be determined simultaneously with x_t, causing some uncertainty in its value at any given location of the route at any given time, the value of $(x_t - x_\mathrm{bg})$ was limited to 0, so that possible negative values would not lead to negative EFs. However, the ELPI+ is an exception for this limiter because x_t denotes the particle number concentration within one size bin, and due to the nature of the ELPI+, it can be negative also. This results from induction currents which are caused by a fastly changing sample. These induction currents, nevertheless, lead to currents to the opposite direction some seconds later, meaning that the sum of the currents (i.e., the concentrations within a bin) from a longer time range have no artifacts due to this induction (because the induction currents will cancel out).

Dilution ratio, DR_t, is calculated in a hybrid way, one of the suggested methods by Leinonen et al. [35], where DR is calculated using CO_2 data for the times when the engine is emitting CO_2 and using the near-wake dilution (NWD) model for the rest. CO_2 data are generally used for DR determination purposes with the equation

$$\mathrm{DR}_t = \frac{\mathrm{CO}_{2,\mathrm{raw},t}}{(\mathrm{CO}_{2,t} - \mathrm{CO}_{2,\mathrm{bg}})} \tag{2}$$

where $\mathrm{CO}_{2,\mathrm{raw},t}$ and $\mathrm{CO}_{2,t}$ are the CO_2 concentrations in the raw exhaust and in the diluted exhaust, respectively, at a given time t, and $\mathrm{CO}_{2,\mathrm{bg}}$ is its background concentration (determined as the median concentration during the background drives similarly to the other pollutants). The values for $\mathrm{CO}_{2,\mathrm{raw},t}$ are obtained from the logged OBD parameters.

The NWD model used for the times when the engine is not emitting, such as in engine motoring events occurring in downhills, uses exhaust dilution mechanics information obtained from the times with CO_2 emissions (also via Eq. (2)). The NWD model is based on the assumption that there is a near-wake region behind a moving vehicle in which the exhaust is fully diluted with the surrounding air. The flow rate of this diluting surrounding air is thought to be the vehicle speed (v_t) multiplied with the area of an imaginary surface that the diluting air passes. This imaginary surface depends mostly on the shape of the rear of the vehicle. The DR at the end of the near-wake region is the flow rate of the diluting air divided by the exhaust flow rate, which leads to the equation

$$\mathrm{DR}_t = \kappa \frac{v_t}{Q_t} + \gamma, \tag{3}$$

where κ is a parameter denoting the area of the imaginary surface and γ is a parameter included to account for any nonidealities in the model. More detailed information on the NWD model and its derivation can be found in Leinonen et al. [35]. Figure S3 and Table S3 of the supplementary material present fittings for the parameters and the parameters with their uncertainties, respectively, of the NWD model (κ and γ) separately for each vehicle. The criteria for using the NWD model, i.e., Eq. (3), rather than Eq. (2) for calculating DR_t are that, firstly, the vehicle speed needs to be higher than 1 km/h, and secondly, that the fuel flow rate needs to be less than 0.1 g/s or the DR_t calculated with Eq. (2) is three times the DR_t calculated with Eq. (3). The latter criterion is used to prevent excessive DRs which may be resulted from situations where the exhaust plume was not captured very well (see the outlying data points with very high DRs in Fig. S3 of the supplementary material), because excessive DRs can lead to significant overestimations of the EFs. In addition, Eq. (3) is used in some relatively rare occasions when the CO_2 analyzer was not functional and when the lambda sensor was not warmed up yet during the first minutes of some experiments with diesel vehicles with SFCSs. The data from the lambda sensor is required for calculating $\mathrm{CO}_{2,\mathrm{raw},t}$ for diesel vehicles. A final limiter to the calculated DR_t, either with Eq. (2) or with Eq. (3), was to limit DR_t within the range of $10 - 10^5$.

A method to estimate the uncertainties in EFs is described in Sect. S3 of the supplementary material. It involves the uncertainty caused by the counting statistics or the noise of the measurement instrument in question and of the CO_2 analyzer, the uncertainties in x_bg and in $\mathrm{CO}_{2,\mathrm{bg}}$, the uncertainties in the NWD model parameters, and the uncertainty of the final DR limiter. The data from different measurement instruments were synchronized using exactly known time stamps of some exceptional experiments, such as directing a short pulse of a lighter emission in the inlet of ATMo-Lab. However, there is still a possibility of less than 2 s of errors in the time synchronizations to the both directions between the instruments and also between the data recorded in ATMo-Lab and in the studied vehicle; this uncertainty is also included in the EF uncertainty calculation.

Because AHs have been running automatically for some parts of the drives with vehicles having the fuel-operated AHs, especially with the lowest temperatures and with SFCSs, it should be noted that the emissions measured with ATMo-Lab also include emissions from the AHs. Because these extra emissions include also CO_2 emissions from the AHs, they cause deviation in the obtained EFs only if the EF of a

given pollutant from the AH differs from the corresponding EF from the engine. This results also from the fact that only the exhaust flow rate from the engine is considered in Q_i in Eq. (1).

3. Results and discussion

Time series of example parameters logged via the OBD port of Skoda Octavia 1 when driving in the lowest outdoor temperature (T =−28 °C) are presented in Fig. S4 of the supplementary material. The example drive is with a preheated–cold start, PHCS, experiment. It can be observed that the coolant temperatures begin from about 40 °C and that the catalyst reaches its operation temperature in 2 min after the engine start.

Figures S5 and S6 of the supplementary material present the time series of the coolant temperature and its increase compared to T for all the drives. It can be observed that, especially with the diesel vehicles, almost the whole drive (13.8 km, about 19 min) is required for the coolant to reach its operation temperature (>60 °C) after cold starts, both after the subfreezing–cold starts, SFCSs, and after the PHCSs. It can also be seen that the fuel-operated AHs with the nominal power of 5 kW and the electric preheater of Audi A6 with the power of 1.2 kW are efficient in heating up the coolant before starting the engine, but they still do not make the reaching of the operation temperature very much faster.

The results on the fuel consumption and emissions are presented and discussed in the following subsections.

3.1. Fuel consumption

Fig. 3 illustrates the dependence of the total fuel consumption for the full drives on outdoor temperature (T) for all studied vehicles. It can be observed that a small effect of T for the gasoline vehicles exists, with the slope of about −0.7 %/°C. For the diesel vehicles, there seems to be no clear effect. In comparison, these fuel consumption slopes in the study with the NEDC cycle by Rautalin [27],Rautalin and Nuottimäki [28] were about −0.8%/°C for both gasoline and diesel vehicles. Nevertheless, the most notable relative difference between the repetition experiments is about 12%: with the PHCSs with Ford Focus, although the difference in T is less than 2 °C (see Table S5 of the supplementary material for numerically expressed results). This implies that this difference in the fuel consumption is caused by weak repeatability of the experiments rather than by the difference in T. A more clear effect on the fuel consumption can be seen with different engine starting types: the differences between SFCSs and hot starts, HSs, (the decrease potential) in the fuel consumption for the full drives are 10%–20%. However, the decrease of the fuel consumption achieved when using a preheater for a cold start is only below 4% with also negative decreases (down to −7%, with VW Transporter) were observed, i.e., the fuel consumption was even higher with PHCSs than with SFCSs. Only vehicles with which preheating benefits were observed are Skoda Octavia 2 and SEAT Alhambra, both having fuel-operated AHs with the nominal power of 5 kW.

Rautalin [27] and Rautalin and Nuottimäki [28] report the fuel consumption decrease potentials for the first 4 km driven in the NEDC cycle, which are on the order of 30%. Similar decrease potentials (21%–41%) are observed also in this study for the combined fuel consumption during the idle period, 1 min, and during the 1st part of the route, 3.2 km (see Table S5 of the supplementary material for the fuel consumption during different segments of the drives). The maximum decrease in this combined fuel consumption achieved with using a preheater is 8.1% but also negative decreases are again observed, whereas Rautalin [27] and Rautalin and Nuottimäki [28] report the decreases of 3.5%–16% achieved with preheaters for the first 4 km in the temperature of −20 °C. Overall, these results from this study are in some cases in line with the study by Rautalin [27] and Rautalin and Nuottimäki [28], but preheating seems to be less beneficial in reducing the fuel consumption according to this study and also not any benefits were observed for some vehicles. Additionally, the benefits are even lower when considering the full route (13.8 km) rather than only the first 4 km, for example. Typical commuting distances in different countries are also closer to 13.8 km than 4 km, denoting that the relative reductions in the fuel consumption achieved with preheating are only minor when looking from the full perspective.

The situation becomes even more noteworthy when considering also the fuel consumption of the AH, which is about 500 g/h for the AHs used in this study. When the 30 min preheating periods with the AHs are also included in the total fuel consumption for the full routes, the fuel consumption was 37% (Skoda Octavia 1) or 26% (Skoda Octavia 2 and SEAT Alhambra) higher in the PHCS drives than in the SFCS drives, even though the fuel consumption decreases of almost 4% were observed for the PHCS drives (including only the engine fuel consumption) with Skoda Octavia 2 and SEAT Alhambra. This confirms that preheating with an AH cannot be justified with increased fuel economy or reduced CO_2 emissions in real-world driving at least under these subfreezing conditions. This also applies to electric preheaters since no decreases in the fuel consumption with preheating were observed with the electric preheater–equipped vehicles of this study. Economic or environmental cost of electric preheaters is out of the scope of this study, but Table S5 of the supplementary material reports also the electric energy consumed by the electric preheaters. Slightly contradictory results on the fuel consumption decrease achieved with electric preheaters were obtained in the study by Rautalin [29], who report 20%–30% decreases with 0.6 kW electric preheaters for the full NEDC cycle with the temperature of −20 °C.

3.2. Particle number, size distribution, and mass emissions

Fig. 4 presents particle number emission factors EF_N for the full drives per driven kilometer for each vehicle, start type, and effective cut-off diameter of the CPCs. Similar plots are also presented separately for different CPCs in Figs. S7–S9 of the supplementary material. It can be observed that, overall, these EFs are significantly higher (up to over 2 orders of magnitude higher) than the PN emissions regulations, which are 6×10^{12} #/km for Ford Focus and 6×10^{11} #/km for the rest. Similar exceedings were observed also, e.g., by Olin et al. [30] in real-world driving under summer conditions. This is partially due to the fact that the measurement system detects both nonvolatile and semivolatile particles, whereas the regulations are only for nonvolatile particles (and only for particles larger than 23 nm). Another observable thing is that the lowest PN emissions in the SFCS drives can be achieved with diesel vehicles without AHs (Audi A6 and VW Transporter). This is probably due to the automatic operation of AHs during driving and thus contributing to the PN emissions. Instead, the only gasoline vehicle without an AH, Ford Focus, emits more than the diesel vehicles probably because it has a GDI engine and is the only vehicle of this study having no particle filter. The use of an AH during driving can basically set a minimum level of emissions under subfreezing conditions that cannot be subceeded even if the engine emissions were totally prevented. See also Tables S6–S8 of the supplementary material, which express the EF data numerically and also include the PN emissions from the 30 min preheating periods for the AH-equipped vehicles. It should be noted that whereas the preheating emissions are relatively not very high compared to the emissions from the full drives and the preheating period is not the most emitting segment in any of the drives, the preheating emissions have been measured with standstill vehicles [26] but the AH emissions during driving may differ from their emissions when preheating because the road draft with very cold outdoor air can enhance nucleation of emitted precursors significantly, leading to much higher PN emission of semivolatile particles.

The PN emissions decrease potential (emissions between the SFCS and HS drives) and the benefit of preheating to PN emissions (emissions between the SFCS and PHCS drives) cannot be estimated—or they do

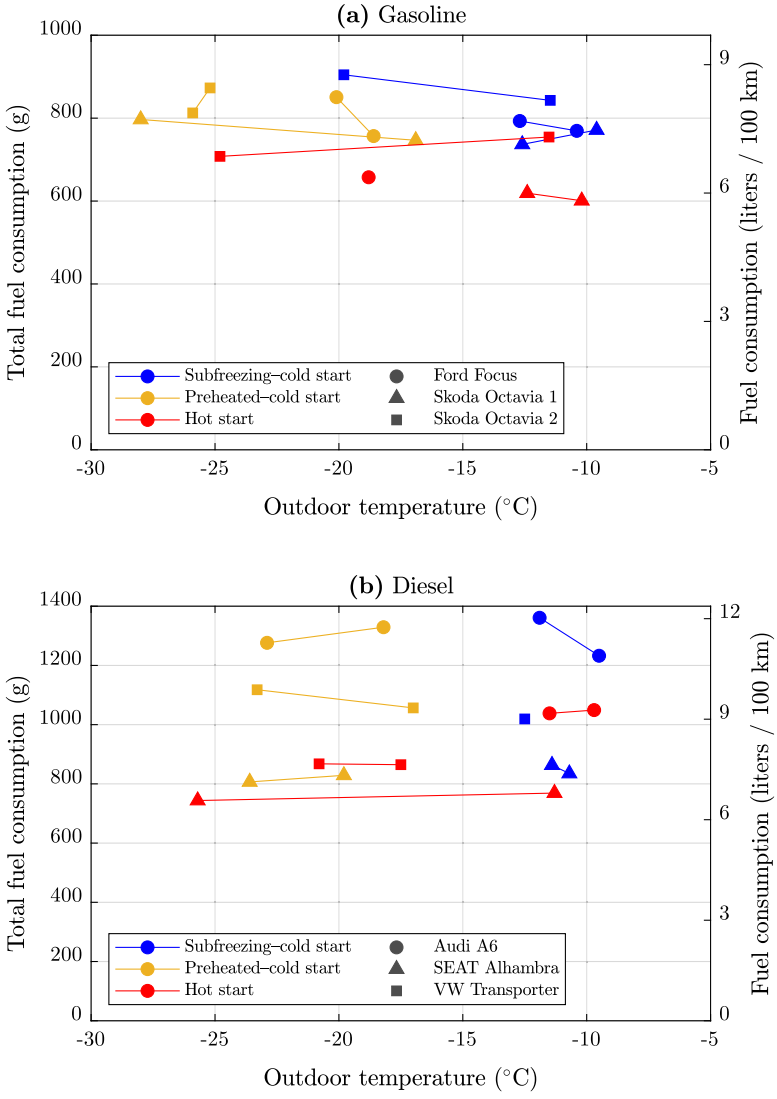

Fig. 3. Fuel consumption of (a) gasoline and (b) diesel vehicles during the drives as a function of outdoor temperature.

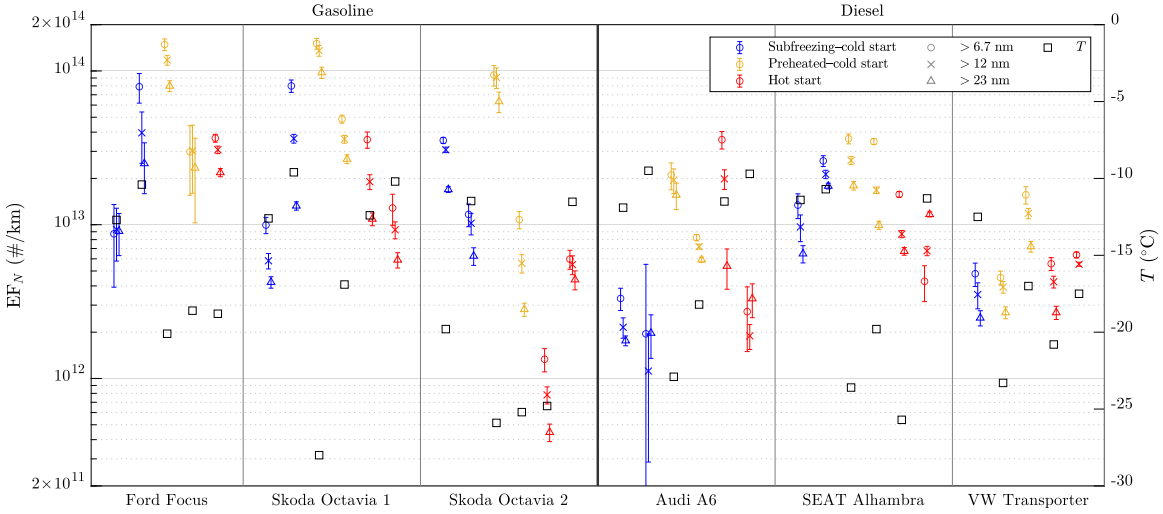

Fig. 4. Particle number emission factors per driven kilometer. Marker types denote the effective cut-off diameters of different CPCs as shown in the legend. The outdoor temperature (T) at the beginning of each drive is also presented. The EFs are also plotted separately for each effective cut-off diameter in Figs. S7–S9 of the supplementary material.

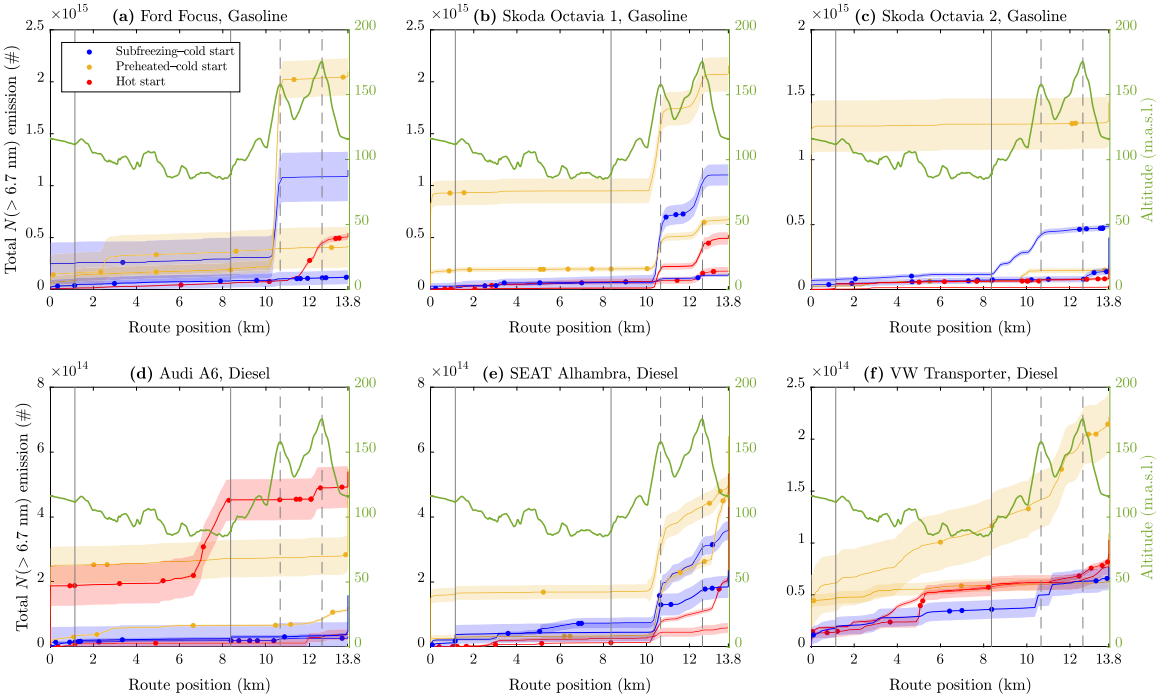

Fig. 5. Total >6.7 nm particle number emission presented cumulatively according to the route position. The shaded areas represent the uncertainties. The green curves represent the altitude profile of the route. The solid vertical lines denote the 30 s stops and the dashed ones the hilltops. The bullet points denote the moments with external disturbances such as other vehicles driving nearby. Similar plots for >12 nm and >23 nm particles are presented in Figs. S21 and S22 of the supplementary material.

not exist—since these EFs do not show any clear trends between the different start types for any of these particle size ranges. Because also the outdoor temperature seems not to have a strong effect on these EFs (see Figs. S15–S17 of the supplementary material), the deviations between the EFs from different drives are possibly caused by reduced repeatability of the experiments, which is generally also expected with this kind of experiments where semivolatile PN emissions are measured by a chasing method in a real-world environment. Although T is probably affecting the formation of delayed primary particle emissions (e.g., via nucleation) the most, other environmental parameters, such as relative humidity and the composition of the background air, can affect too. On the other hand, the uncertainties of the EFs are not extensively high, providing confidence in the results. Therefore, it can be concluded that controlling the PN emissions is not possible with using preheaters at least under the studied conditions and that preheating and additional AH operation during driving can even enlarge the emissions with fuel-operated heaters.

Fig. 5 presents PN emissions of >6.7 nm particles, N(>6.7 nm), cumulatively according to the route position (similar plots for >12 and >23 nm particles are shown in Figs. S21 and S22 of the supplementary material). Firstly, it can be observed that in some cases the idle period emits a notable number of particles compared to the full drive (the line beginning from a level clearly above zero). Secondly, it can be observed that in many cases (especially with Skoda Octavia 1 and SEAT Alhambra) a significant number of particles are emitted when driving uphill the tall hills in the 4th part of the route (increasing trends right before the dashed vertical lines). SEAT Alhambra and VW Transporter seem to emit a high number of particles also when driving downhill (increasing trends also after the dashed lines). For SEAT Alhambra, this can also be seen from Tables S6–S8 of the supplementary material with most of the PN emissions observed in the 4th part of the route, where the tall hills exist. If the emissions from this hilly 4th part is disregarded, the most of the emission is observed either during the idle period or in the 1st part of the route in almost every case. Finally, it can be observed that external disturbances, such as other vehicles driving nearby or some nearby houses with wood burning emissions from their stacks, do not cause any significant misinterpretations in the results, as these disturbances shown with the bullet points in the cumulative emission plots do mainly not lead to any extensive disturbances in the cumulative trends at their locations.

Particle size distributions, $\mathrm{d}N/\mathrm{d}\log D_\mathrm{p}$, emitted by the studied vehicles are mainly skewed so that the emitted number of smaller particles is higher compared to the larger particles, as can be seen from Fig. 4 with clear differences between the EF_N for different particle size ranges and from Fig. 6 presenting the emission factor particle size distributions measured with the ELPI+, $\mathrm{dEF}_{N(\mathrm{ELPI+})}/\mathrm{d}\log D_\mathrm{p}$. Some hints of bimodal size distributions can be interpreted from $\mathrm{dEF}_{N(\mathrm{ELPI+})}/\mathrm{d}\log D_\mathrm{p}$ from some drives: a soot mode near D_p of 100 nm and a nucleation mode with somewhat smaller sizes closer to 10 nm. Whereas the soot mode is typically associated with nonvolatile particles of primary emission, the nucleation mode is associated with semivolatile particles formed as delayed primary emissions; however, also the nonvolatile particles are presumed to be covered with semivolatile material condensed onto them upon exhaust cooling. As expected, the emitted particles with soot mode–like D_p are the highest for Ford Focus being the only studied vehicle without a particle filter. The emitted particles with nucleation mode–like D_p, instead, seem to be higher for the gasoline vehicles than for the diesel vehicles. No clear effect of the engine start type on $\mathrm{dEF}_{N(\mathrm{ELPI+})}/\mathrm{d}\log D_\mathrm{p}$ can be observed.

When looking at the total PM emissions calculated from the ELPI+ data, the emission factors for the full drives ($\mathrm{EF}_{M(\mathrm{ELPI+})}$) shown in Fig. 7, the decrease potential of PM emissions are observable (see also Table S9 of the supplementary material for numerical representation of the EFs and for the PM emissions from the AHs during preheating). There are decrease potentials of 25%–85% for the all gasoline vehicles and for SEAT Alhambra, but they were not observed for the rest of the vehicles. However, the benefit to PM emission reductions from using a preheater were observed only for Skoda Octavia 2 (72% reduction) and for SEAT Alhambra (24% reduction); these values take also the PM emissions from the 30 min preheating period into account. When considering only the emissions from the idle and from the 1st part of the route, the decrease potentials up to 99% (with Ford Focus) were

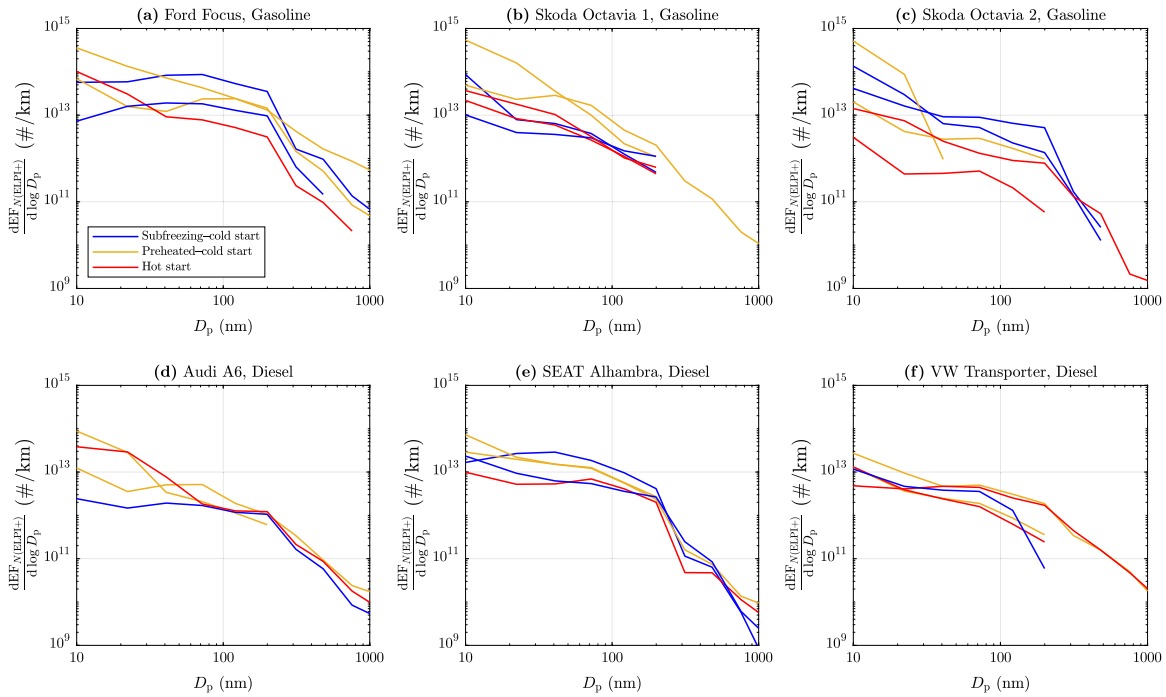

Fig. 6. Emission factor particle size distributions for the full drives measured with ELPI+. The distributions are shown only for the first size bins with positive EFs (possible negative EFs are caused by the unknown particle density in the data inversion).

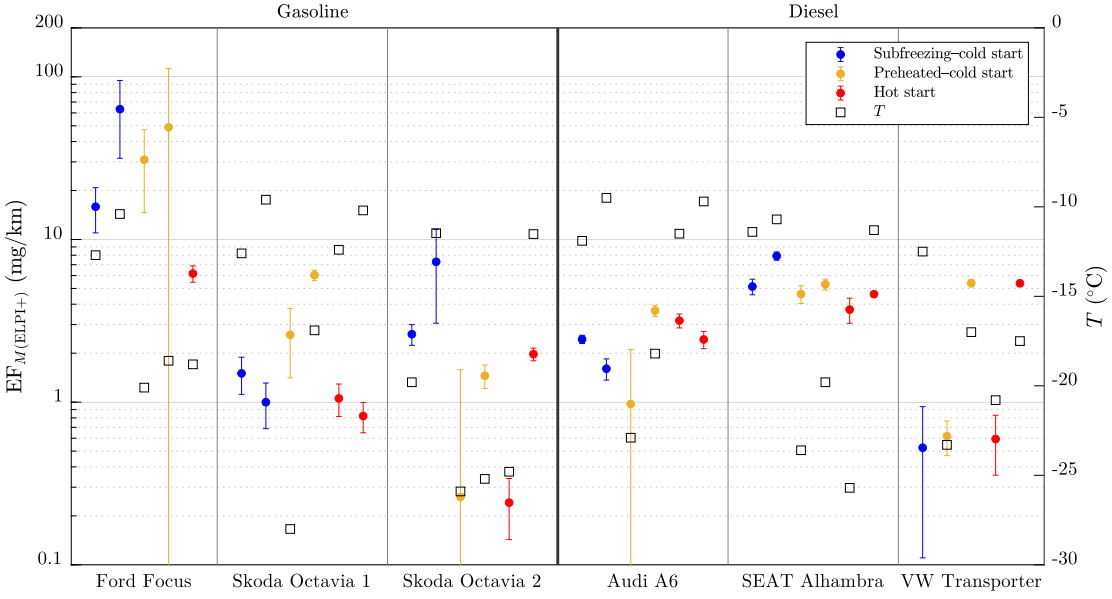

Fig. 7. Mass emission factors of <600 nm particles per driven kilometer measured with ELPI+. The outdoor temperature (T) at the beginning of each drive is also presented.

observed. However, the benefits to the emission reductions for these segments from using a preheater were again only observed for Skoda Octavia 2 (86% reduction) and for SEAT Alhambra (47% reduction). For comparison, these benefits to the PM emission reductions from the first 4 km driving in the NEDC cycle with the temperature of −20 °C reported by Rautalin [27],Rautalin and Nuottimäki [28] were 52%–78% for gasoline vehicles, which are in line with the results of this study only in the case of Skoda Octavia 2. It is also notable that no benefits to these emission reductions were observed with the vehicles having an electric preheater in this study, even for the combined segments of idle period and the 1st part of the route. It is also noteworthy to mention that no clear effect of T on M(ELPI+) emissions was observed (see Fig. S18 of the supplementary material).

Unlike in the case of PN emissions exceeding their regulation limits by even orders of magnitude, similar exceedings are not observed with the PM emissions. However, as the limit in the regulations is 5 mg/km, Ford Focus exceeds this limit with all drives, up to an order of magnitude, and some minor exceedings can be observed with some of the drives with the other vehicles. It can be observed from the cumulative M(ELPI+) emission plots in Fig. S23 and from the numeric EF data for the different segments of the drives in Table S9 of the supplementary material that the highest contribution to the total M(ELPI+) emission was during idling with Ford Focus (except with the HS) and during the 4th part of the drive with SEAT Alhambra, but are scattered between the segments for the rest of the vehicles.

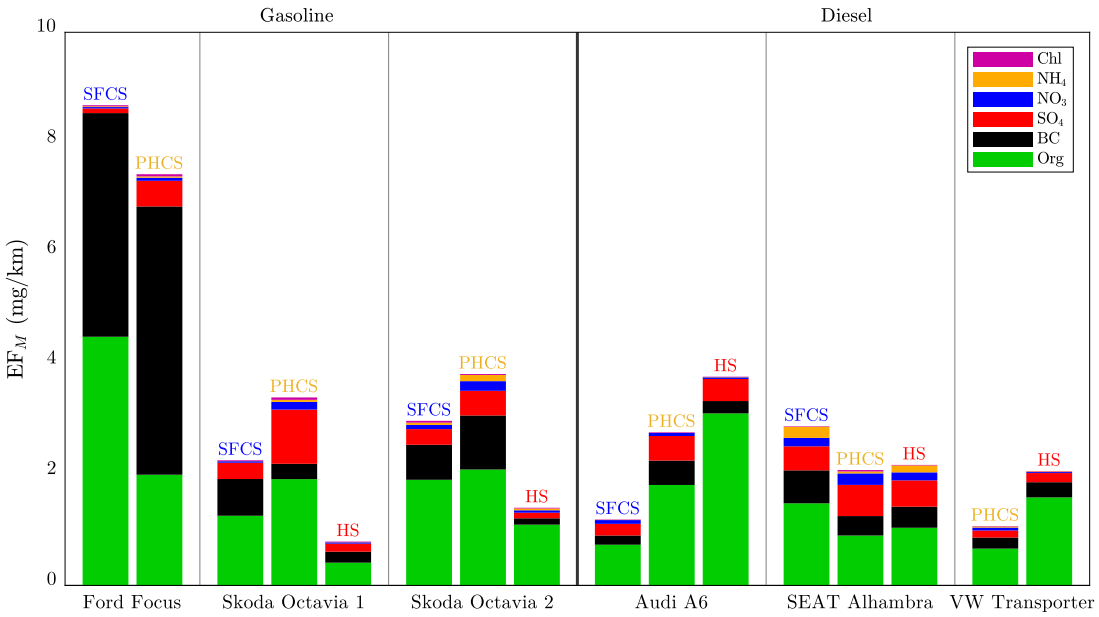

Fig. 8. Chemically resolved particle mass emission factors. The EFs are also presented separately for each species, together with their uncertainties, in Figs. S24–S28 of the supplementary material and in Fig. 9.

3.3. Chemically resolved particle mass emissions

EFs for different components of PM (EF_M) are presented in Fig. 8. As discussed previously, it can be observed that emitted particles consist of both nonvolatile and semivolatile parts, with the major fraction in PM being semivolatile (except the PHCS drive with Ford Focus). The nonvolatile part from these components is black carbon, BC, (measured with the AE33) whereas the semivolatile part consists of the rest of the components (measured with the SP-AMS), of which organics, Org, is the main component. It can also be observed that, for the gasoline vehicles, the BC emissions from the HS drives are clearly lower than from the SFCS drives (see also Fig. 9) and that preheating can give some benefits to reducing BC emissions, as was the case with the M(ELPI+) emissions too. Note that EF_{BC} cannot be directly compared with $EF_{M(ELPI+)}$ (e.g., for estimating the fraction of BC in aerosol) because they are determined with different time resolutions. Higher time resolution typically leads to higher EFs because instantaneous EFs are typically positively correlated with exhaust flow rate. In this study, e.g., $EF_{M(ELPI+)}$ are about 20% higher, in median, by using the time resolution of 1 s compared to if they were determined by using the time resolution of 23 s (like for BC). However, for Ford Focus, this percentage can be up to 800%, which is the reason why $EF_{M(ELPI+)}$ (in Fig. 7) seem to be about an order of magnitude higher than EF_{BC} (in Fig. 9). Similarly to M(ELPI+) emissions, no clear effect of T on BC emissions was observed (see Fig. S19 of the supplementary material). Because there were no repetition experiments with the SP-AMS, repeatability of these results cannot be estimated. As can be seen from the cumulative emissions plots in Figs. S24–S29 and from the numeric EF_M data in Tables S10–S15 of the supplementary material, most of the BC emissions were released during the first minutes but the nonvolatile particle emissions, such as Org, are more pronounced during the ends of the drives.

For the diesel vehicles, no clear dependency of the engine start type on the BC emissions is observed. The Org emissions behave also differently for them compared to the gasoline vehicles: highest Org emissions were observed with the HSs, except in the case of SEAT Alhambra. Notable for SEAT Alhambra is also that it has the highest particle ammonium mass, NH_4, emissions, mostly emitted when driving the tall hills uphill during the 4th part of the route, but NH_4 emissions from Skoda Octavia 2 are also close to these values (see Fig. S27 of the supplementary material). Higher NH_4 emissions from SEAT Alhambra can be explained with ammonia slip, that can occur with SCR-equipped vehicles when ammonia (NH_3) remains unreacted in the SCR system, e.g., with too high instantaneous urea injection or with too low temperatures leading to lower reactivity of NH_3.

By concluding the chemically resolved PM emission results, any significant benefits to reduce these emissions or to make the chemical composition of particles somehow environmentally more friendly cannot be obtained with preheating these vehicles when driving in a real-world environment under the studied subfreezing conditions.

3.4. Nitrogen oxides emissions

Fig. 10 presenting the EFs of nitrogen oxides, NO_x, shows that the NO_x emissions are substantially higher for the diesel vehicles (especially Audi A6 and SEAT Alhambra) and that all vehicles exceeded their NO_x regulation limits with most of the drives. Whereas the NO_x regulation limits for these gasoline vehicles are 60 mg/km, these vehicles exceeded the limits by the factors of 1.4–6.2, with the exception of the HS drives with the both Skoda Octavias, with which the limits were not exceeded (see also Table S16 of the supplementary material for the numerical representation of the EFs). The NO_x regulation limits for the diesel vehicles are 180 mg/km for Audi A6 and SEAT Alhambra and 80 mg/km for VW Transporter. These limits were exceeded by the factors of 1.3–21, the smallest exceedings observed with VW Transporter and the largest ones with Audi A6. It is noteworthy to mention that only SEAT Alhambra has the EA189 engine model that has been connected with excessive NO_x emissions in the Dieselgate scandal; however, it has received the official software update that should fix the excessive NO_x emissions. There are also no aware end user manipulation software updates made for any of the vehicles, which could cause elevated NO_x emissions. The highest NO_x emissions from Audi A6 are obvious because it is the only diesel vehicle from this set of vehicles without a SCR system. High NO_x emissions from SEAT Alhambra can probably be explained with some underperformance of its SCR system, as there were some NH_4 emissions which can be linked to ammonia slip. One of the reasons for the excessive NO_x emissions from the diesel vehicles can be the temperature range of this study, because some hints on increased NO_x emissions with decreased T are observable for diesel vehicles (see Fig. S20 of the supplementary material). No similar effect of T on the

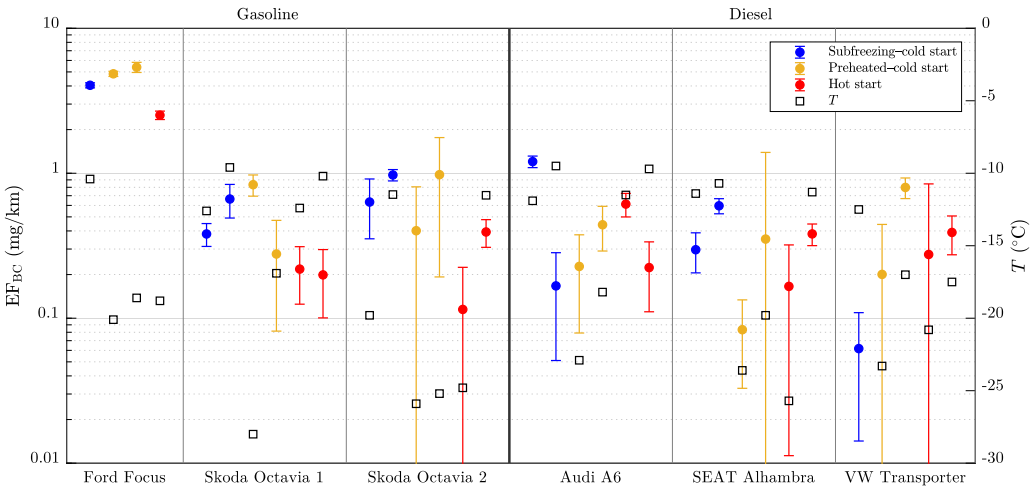

Fig. 9. Black carbon mass emission factors per driven kilometer. The outdoor temperature (T) at the beginning of each drive is also presented.

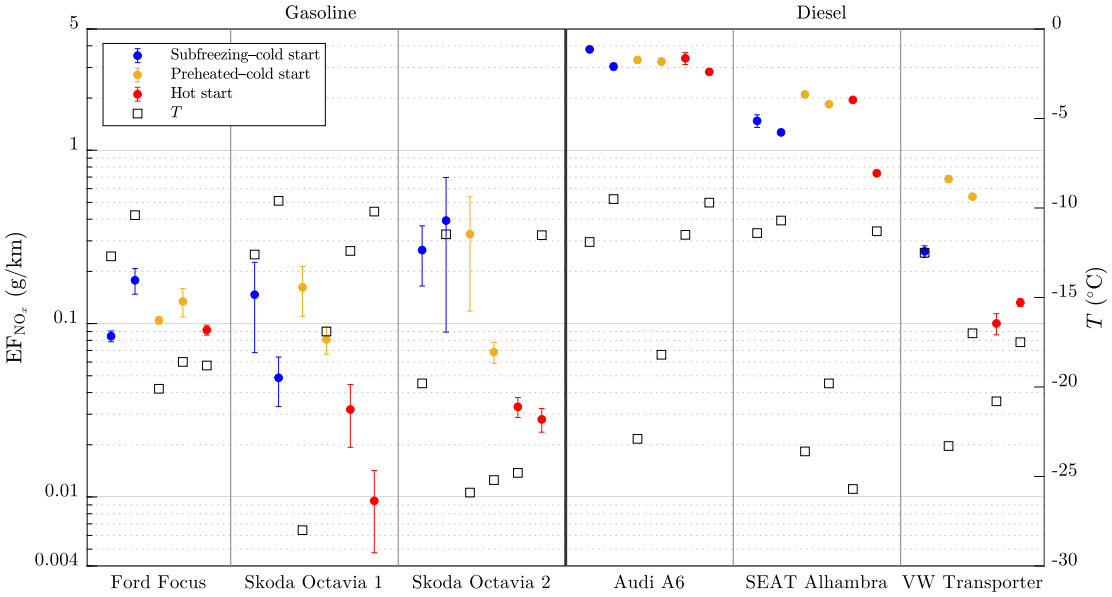

Fig. 10. Nitrogen oxides emission factors per driven kilometer.

NO_x emissions from the gasoline vehicles is seen, although Rautalin and Nuottimäki [28] observed this effect for both gasoline and diesel vehicles.

The decrease potentials of the total NO_x emissions from the full drives were observed with the all vehicles: 30%–90% for the gasoline vehicles and 1%–55% for the diesel vehicles. However, the benefits to the reduced NO_x emissions from preheating were observed only for Ford Focus, Skoda Octavia 2, and Audi A6, of which only with Skoda Octavia 2 a remarkable benefit (41% reduction) is observed. However, the dependency of T on the NO_x emissions from the diesel vehicles may hinder some of the observable benefits from preheating for the diesel vehicles because T was generally lower during the PHCS experiments. For comparison, Rautalin [29] observed about 40%–50% reductions of NO_x emissions from the NEDC cycle driving with electrical preheating.

Although the NO_x emissions from the gasoline vehicles were about an order of magnitude lower than from the diesel vehicles, a high contribution to the total NO_x emitted can originate from the AH use as the NO_x emissions from the AHs of gasoline vehicles are even somewhat higher than of the diesel vehicles. The segment with the highest NO_x emissions from the full drive including preheating was preheating for two of the four PHCS experiments with the both Skoda Octavias. Taking this 30 min preheating period into account, the preheating benefit to NO_x emission reduction for Skoda Octavia 2 decreases from 41% to 15%.

As can be seen from the cumulative NO_x emission plots in Fig. S30 of the supplementary material, the gasoline vehicles show pronounced NO_x emissions from idling, whereas the diesel vehicles seem to be more like continuous NO_x emitters without clear effects from the driving situation (although the VW Transporter data show some elevated emissions when driving on the tallest hills).

4. Conclusions

The results showed that, especially with the studied diesel vehicles, almost the whole drive (13.8 km, about 19 min, 50 ± 20 km/h) was required for the engine coolant to reach its operation temperature (>60 °C) after cold-starting the engine under the studied Finnish winter conditions (−28 … -10 °C). However, powerful preheaters (>1 kW) were efficient in heating up the coolant before starting the engine, but they did not make the reaching of the operation temperature very much faster. The increased starting temperatures enhance mostly the comfortability of the vehicle users, such as by providing a warmer cabin

and by melting down possible ice from the windows, and may prevent excessive engine wear during cold starts.

Potentials to decrease the fuel consumption for the full drives with preheating of 10%–20% were observed by comparing the total fuel consumptions for the drives with the engine being cold (called subfreezing–cold start, SFCS) or hot (called hot start, HS) when starting. However, preheating the engines before starting (called preheated–cold start, PHCS) resulted in fuel savings of only less than 4%, when compared to the SFCS drives. Only two of the six studied vehicles, both having fuel-operated auxiliary heaters (AHs), showed any fuel savings from preheating. These potentials and benefits from preheating to fuel economy become roughly double when only the idle period of 1 min and the first 3.2 km driving are considered. Typical commuting distances are, however, closer to the full 13.8 km drive, making the benefit of preheating to fuel economy relatively small. These values for increased fuel economy, however, do not take the fuel or electricity consumption of the preheaters into account. The fuel-operated AHs have a fuel consumption comparable to an idling engine, and taking their total fuel consumption from a typical heating period of 30 min into account, all fuel savings achieved with preheating cancel out, leading to 26%–37% higher total fuel consumption—and thus CO_2 emissions—from the drives where preheating was applied before the engine start. This result confirms that the justification of the fuel-operated AH usage with increased fuel economy or reduced CO_2 emissions do not hold in real-world driving under subfreezing conditions, which is against a common thought of their usage. However, if assessing a full life cycle of a vehicle, significant benefits from preheating could be obtained by increased life time of the lubricant and the engine itself because engine wear is presumably minimized when the number of SFCSs is minimized.

Similarly to the total fuel consumption, no notable benefits to decrease PN emissions with preheating were detected. The emission factors of PN including all particles (also semivolatile) were observed to be up to 2 orders of magnitude higher than the PN emission limits in the regulations for the type-approval of vehicles, which is partly explained with the fact that the PN regulations include only nonvolatile particles larger than 23 nm. The lowest PN emissions were detected with diesel vehicles without fuel-operated AHs, which may be explained with the emissions of the AHs during driving, because they also automatically operate during driving when additional heat is needed for the engine or for the cabin.

Unlike in the case of the PN emissions, the emissions of PM, BC, and NO_x showed clear decrease potentials for most of the vehicles. The PM and BC emissions were lower in the HS drives than in the SFCS drives especially for the gasoline vehicles, with the highest PM decrease potentials of 85% for the full drives and 99% for the idle period and the 1st part of the route. The decrease potentials for the NO_x emissions were 1%–90%. However, the benefits achieved with preheating to decrease the PM emissions were observed only for one gasoline vehicle, with a reduction of 72%, and for one diesel vehicle, with a reduction of 24%. For the BC emissions, only minor benefits from preheating were observed. For the NO_x emissions, remarkable benefits from preheating were observed only with this gasoline vehicle, with the reduction of 41%. Additionally, this benefit achieved with using the AH for preheating decreases to only 15% when the NO_x emissions from the AH are taken into account, since they have considerable NO_x emissions as well, especially with the gasoline vehicles. Notable is that no significant benefits from electrical preheaters to the fuel consumption or to any type of emissions were observed.

For the diesel vehicles, the contribution of the AH to the total NO_x emissions is not as high as for the gasoline vehicles, because the NO_x emissions from the diesel vehicles were significantly higher. While all the studied vehicles showed NO_x emissions higher than the regulation limits, the highest exceedings were observed with the diesel vehicles, up to a factor of 21. Noteworthy is that the NO_x emissions from one diesel vehicle exceeded the regulation limit with a factor of 12 even though it is equipped with the SCR system. This implies that the SCR system is not fully functionable under subfreezing conditions. In addition, a possible ammonia slip of this SCR system was observed, as the highest NH_4 emissions (particle ammonium mass) were detected with this vehicle.

In conclusion, justification of preheating with better fuel economy and lower emissions during driving seems not to hold very well in real-world driving under the studied subfreezing conditions. Types of driving routes different from the studied route and assessing the full life cycles of the vehicles may, however, display slightly different conclusions. Although the studied emissions including particle and NO_x emissions showed some benefits from preheating with fuel-operated AHs to reduced emissions during driving, the benefits become much smaller or even cancel out when considering also the fuel consumption and the emissions of the AH during its preheating period. There can, however, be other emissions not measured in this study, e.g., specific hydrocarbons, which could involve larger benefits from preheating. It should be noted that these specific emissions from fuel-operated AHs can yet be high as well and can even cancel the preheating benefits out.

CRediT authorship contribution statement

Miska Olin: Writing – review & editing, Writing – original draft, Visualization, Supervision, Resources, Project administration, Methodology, Investigation, Formal analysis, Data curation, Conceptualization. **Ville Leinonen:** Writing – review & editing, Resources, Methodology, Investigation, Formal analysis. **Sampsa Martikainen:** Writing – review & editing, Investigation, Conceptualization. **Ukko-Ville Mäkinen:** Formal analysis, Data curation. **Henri Oikarinen:** Writing – review & editing. **Santtu Mikkonen:** Writing – review & editing, Supervision, Resources, Project administration, Methodology, Investigation, Funding acquisition, Conceptualization. **Panu Karjalainen:** Writing – review & editing, Supervision, Resources, Project administration, Methodology, Investigation, Funding acquisition, Data curation, Conceptualization.

Declaration of competing interest

The authors declare that they have no known competing financial interests or personal relationships that could have appeared to influence the work reported in this paper.

Data availability

Data will be made available on request.

Acknowledgments

This research is a campaign of the “AHMA” project funded by the Jane and Aatos Erkko’s Foundation, Finland and of the Academy of Finland project “EFFi” (grant no. 322120). S.Ma. acknowledges funding from the Kone Foundation, Finland. S.Mi. is supported by the Academy of Finland competitive funding to strengthen university research profiles (PROFI) for the University of Eastern Finland (grant no. 325022). P.K. acknowledges funding from Tampere Institute for Advanced Study (Tampere IAS), Finland. This research has also received support from the Academy of Finland Flagship Programme “ACCC”, Finland (grant nos. 337550 and 337551). Tampere University’s mobile laboratory, ATMo-Lab, contributes to the INAR RI and ACTRIS infrastructures. The following persons assisted in the experiments are also acknowledged: Anssi Arffman, Leonardo Negri, Markus Nikka, and Harri Timonen.

Appendix A. Supplementary data

Supplementary material related to this article can be found online at https://doi.org/10.1016/j.apenergy.2023.121805.

References

[1] Kittelson D, Johnson J, Watts W, Wei Q, Drayton M, Paulsen D. Diesel aerosol sampling in the atmosphere. SAE J-Automot Eng 2000;2000–01–2212.

[2] Wehner B, Birmili W, Gnauk T, Wiedensohler A. Particle number size distributions in a street canyon and their transformation into the urban-air background: measurements and a simple model study. Atmos Environ 2002;36(13):2215–23.

[3] Hietikko R, Kuuluvainen H, Harrison RM, Portin H, Timonen H, Niemi JV, et al. Diurnal variation of nanocluster aerosol concentrations and emission factors in a street canyon. Atmos Environ 2018;189:98–106.

[4] Olin M, Kuuluvainen H, Aurela M, Kalliokoski J, Kuittinen N, Isotalo M, et al. Traffic-originated nanocluster emission exceeds H_2SO_4-driven photochemical new particle formation in an urban area. Atmos Chem Phys 2020;20(1):1–13.

[5] Olin M, Patoulias D, Kuuluvainen H, Niemi JV, Rönkkö T, Pandis SN, et al. Contribution of traffic-originated nanoparticle emissions to regional and local aerosol levels. Atmos Chem Phys 2022;22(2):1131–48.

[6] Lintusaari H, Kuuluvainen H, Vanhanen J, Salo L, Portin H, Järvinen A, et al. Sub-23 nm particles dominate non-volatile particle number emissions of road traffic. Environ Sci Technol 2023;57:10763–72.

[7] DieselNet. 2022 URL https://dieselnet.com. [last accessed 19 April 2022].

[8] Karjalainen P, Rönkkö T, Pirjola L, Heikkilä J, Happonen M, Arnold F, et al. Sulfur driven nucleation mode formation in diesel exhaust under transient driving conditions. Environ Sci Technol 2014;48(4):2336–43.

[9] Rönkkö T, Virtanen A, Vaaraslahti K, Keskinen J, Pirjola L, Lappi M. Effect of dilution conditions and driving parameters on nucleation mode particles in diesel exhaust: Laboratory and on-road study. Atmos Environ 2006;40(16):2893–901.

[10] Rönkkö T, Kuuluvainen H, Karjalainen P, Keskinen J, Hillamo R, Niemi JV, et al. Traffic is a major source of atmospheric nanocluster aerosol. Proc Natl Acad Sci USA 2017;114(29):7549–54.

[11] Preble CV, Dallmann TR, Kreisberg NM, Hering SV, Harley RA, Kirchstetter TW. Effects of particle filters and selective catalytic reduction on heavy-duty diesel drayage truck emissions at the Port of Oakland. Environ Sci Technol 2015;49(14):8864–71.

[12] Khalek IA, Blanks MG, Merritt PM, Zielinska B. Regulated and unregulated emissions from modern 2010 emissions-compliant heavy-duty on-highway diesel engines. J Air Waste Manage 2015;65(8):987–1001.

[13] Wihersaari H, Pirjola L, Karjalainen P, Saukko E, Kuuluvainen H, Kulmala K, et al. Particulate emissions of a modern diesel passenger car under laboratory and real-world transient driving conditions. Environ Pollut 2020;265:114948.

[14] Alkidas AC. Combustion advancements in gasoline engines. Energy Convers Manage 2007;48(11):2751–61.

[15] Aakko P, Nylund N-O. Particle emissions at moderate and cold temperatures using different fuels. SAE J-Automot Eng 2003;2003–01–3285.

[16] Mohr M, Forss A-M, Lehmann U. Particle emissions from diesel passenger cars equipped with a particle trap in comparison to other technologies. Environ Sci Technol 2006;40(7):2375–83.

[17] Braisher M, Stone R, Price P. Particle number emissions from a range of European vehicles. SAE J-Automot Eng 2010;2010–01–0786.

[18] Reiter MS, Kockelman KM. The problem of cold starts: A closer look at mobile source emissions levels. Transp Res D 2016;43:123–32.

[19] Drozd GT, Zhao Y, Saliba G, Frodin B, Maddox C, Weber RJ, et al. Time resolved measurements of speciated tailpipe emissions from motor vehicles: Trends with emission control technology, cold start effects, and speciation. Environ Sci Technol 2016;50(24):13592–9.

[20] Saliba G, Saleh R, Zhao Y, Presto AA, Lambe AT, Frodin B, et al. Comparison of gasoline direct-injection (GDI) and port fuel injection (PFI) vehicle emissions: Emission certification standards, cold-start, secondary organic aerosol formation potential, and potential climate impacts. Environ Sci Technol 2017;51(11):6542–52.

[21] Weilenmann M, Favez J-Y, Alvarez R. Cold-start emissions of modern passenger cars at different low ambient temperatures and their evolution over vehicle legislation categories. Atmos Environ 2009;43(15):2419–29.

[22] Bielaczyc P, Szczotka A, Woodburn J. The effect of a low ambient temperature on the cold-start emissions and fuel consumption of passenger cars. Proc Inst Mech Eng 2011;225(9):1253–64.

[23] Surcel M-D. Evaluation of the effect of ambient conditions on the fuel consumption of commercial vehicles. In: WCX SAE world congress experience. 2022, SAE Technical Paper.

[24] Roberts A, Brooks R, Shipway P. Internal combustion engine cold-start efficiency: A review of the problem, causes and potential solutions. Energy Convers Manage 2014;82:327–50.

[25] Karjalainen P, Nikka M, Olin M, Martikainen S, Rostedt A, Arffman A, et al. Fuel-operated auxiliary heaters are a major additional source of vehicular particulate emissions in cold regions. Atmosphere 2021;12:1105.

[26] Oikarinen H, Olin M, Martikainen S, Leinonen V, Mikkonen S, Karjalainen P. Particle number, mass, and black carbon emissions from fuel-operated auxiliary heaters in real vehicle use. Atmos Environ X 2022;16:100189.

[27] Rautalin J. Moottorin esilämmityksen vaikutukset [Ph.D. thesis], Helsinki, Finland: Metropolia University of Applied Sciences; 2013, URL http://urn.fi/URN:NBN:fi:amk-2013100315819.

[28] Rautalin J, Nuottimäki J. Henkilöauton moottorin esilämmityksen vaikutus päästöihin ja energian kulutukseen. Technical report VTT-R-06328-13, VTT; 2013.

[29] Rautalin J. Defa energy test. Technical report VTT-CR-01725-15, VTT; 2015.

[30] Olin M, Oikarinen H, Marjanen P, Mikkonen S, Karjalainen P. High particle number emissions determined with robust regression plume analysis (RRPA) from hundreds of vehicle chases. Environ Sci Technol 2023;57(24):8911–20.

[31] DeCarlo PF, Kimmel JR, Trimborn A, Northway MJ, Jayne JT, Aiken AC, et al. Field-deployable, high-resolution, time-of-flight aerosol mass spectrometer. Anal Chem 2006;78(24):8281–9.

[32] Onasch TB, Trimborn A, Fortner EC, Jayne JT, Kok GL, Williams LR, et al. Soot particle aerosol mass spectrometer: Development, validation, and initial application. Aerosol Sci Technol 2012;46(7):804–17.

[33] Middlebrook AM, Bahreini R, Jimenez JL, Canagaratna MR. Evaluation of composition-dependent collection efficiencies for the aerodyne aerosol mass spectrometer using field data. Aerosol Sci Technol 2012;46(3):258–71.

[34] Carslaw DC, Farren NJ, Vaughan AR, Drysdale WS, Young S, Lee JD. The diminishing importance of nitrogen dioxide emissions from road vehicle exhaust. Atmos Environ X 2019;1:100002.

[35] Leinonen V, Olin M, Martikainen S, Karjalainen P, Mikkonen S. Challenges and solutions in determining dilution ratios and emission factors from chase measurements of passenger vehicles. Atmos Measur Technol 2023 [in review].